Cu₂SnS₃ based thin film solar cells from chemical spray pyrolysis

Mohamed H. Sayed[a],[*],[1], Erika V.C. Robert[b], Phillip J. Dale[b], Levent Gütay[a]

[a] *Laboratory for Chalcogenide Photovoltaics, Energy and Semiconductor Research Department, Institute of Physics, University of Oldenburg, D-26111 Oldenburg, Germany*
[b] *Physics and Materials Science Research Unit, University of Luxembourg, L-4422 Belvaux, Luxembourg*

ARTICLE INFO

ABSTRACT

A simple and eco-friendly method for solution processing of Cu_2SnS_3 p-type semiconductor absorbers using a water-based precursor solution is presented. Cu_2SnS_3 layers were processed by chemical spray pyrolysis deposition of the precursor solution onto Mo-coated glass substrates at 350 °C. The as-prepared layers were placed inside a graphite susceptor with S and SnS powders and were annealed in a tube furnace at 550 °C. The impact of the annealing step on structural, morphological and device characteristics of the prepared layers was studied.

The as-prepared layers were crack-free with fine grains and dominant tetragonal Cu_2SnS_3 structure. A denser and compact Cu_2SnS_3 layer with larger grains was formed upon annealing accompanied by a structural phase transition from the tetragonal polymorph to the monoclinic phase. The as-prepared Cu_2SnS_3 layers showed no photovoltaic activity, whereas the annealed layers showed a device efficiency of 0.65%. A short air annealing of the complete Cu_2SnS_3 device at 250 °C improved the overall device performance and increased the device efficiency to 1.94%. Mechanical removal of shunt paths led to Cu_2SnS_3 device with 2.28% efficiency.

1. Introduction

Thin film photovoltaics technology is currently dominated by the p-type $Cu(In,Ga)(S,Se)_2$ semiconductor, which when imbedded as an absorber layer, produces up to 22.9% efficient solar cells [1,2]. However, the high costs of In and Ga suggest to pursue for alternative materials with cheaper elements, such as Zn and Sn.

The p-type $Cu_2ZnSn(S,Se)_4$ semiconductor thus became an optimum alternative but up to now devices have not reached any efficiency higher than 12.6% [3], due to the higher number of chemical elements leading to the difficulty to grow single phase material, to the presence of disorder on the cation sites and to the formation of detrimental amounts of secondary phases and deep defects [4,5].

In order to reduce the number of chemical elements and the complexity of the semiconductor, focus increased on Cu_2SnS_3 in the last years, also a p-type semiconductor ternary with a bandgap between 0.9 and 1.4 eV, which is suited for solar energy conversion in single pn junction and/or bottom cell in tandem devices [6,7]. Thin films of Cu_2SnS_3 were produced from both vacuum based methods and less expensive non-vacuum chemical methods, such as spray pyrolysis [8,9]. A device efficiency of 4.29% was obtained with an absorber prepared from vacuum evaporated precursors which were further annealed in a sulfur atmosphere above 500 °C [10]. Na doping increased the

efficiency to 4.6% [11] which is the highest efficiency reported up to now. However, devices produced from chemically synthesized precursors were reported to show lower performances below 3% when electrodeposited [12] or down to below 1% from spray pyrolysis [13]. While electrodeposited precursors are generally annealed above 500 °C in the presence of sulfur and SnS, processing temperatures and conditions of spray pyrolysed precursors vary between simple heating at 350 °C during deposition [14] and additional heating steps at higher temperatures in vacuum or only in the presence of sulfur [15]. One could attribute the lower performances to the increased difficulty to produce films of uniform composition and morphologies when using chemical methods. Additionally, Cu_2SnS_3 is known as a polymorphic material whose structural and optoelectronic properties vary upon synthesis method, particularly prone to disorder when low annealing temperatures are employed [16]. Tetragonal, cubic and monoclinic polymorphs of Cu_2SnS_3 are reported. In this work we present the effect of a high temperature annealing step on films deposited by spray pyrolysis. In the first part we analyse the crystallographic, vibrational and morphological properties of the as-prepared thin films and then study them after annealing. The second part shows the device results of these same films imbedded into complete solar cells.

---

* Corresponding author.
E-mail address: mohamed.mohamed@uni-oldenburg.de (M.H. Sayed).
[1] Current address: Solid State Physics Department, National Research Centre, 12622 Cairo, Egypt

2. Experimental details

Precursor Cu_2SnS_3 layers were deposited onto the molybdenum coated soda lime glass (Mo-SLG) substrates using the chemical spray pyrolysis method. The precursor solution was prepared with 5.7 mM copper nitrate (puriss. p.a., 99–104%, Sigma Aldrich), 3.7 mM tin methanesulfonate (50 wt% in H_2O, Sigma Aldrich) and 40 mM thiourea (ACS reagent, ≥99.0%, Sigma Aldrich), which were dissolved separately in distilled water and mixed together before spraying. An excess of thiourea was used in order to compensate for the possible loss of sulfur and to inhibit the formation of metal oxides during the spraying process. A few drops of concentrated nitric acid (65%, Fisher Scientific) were added to adjust the pH value around 2 to avoid the precipitation of the final precursor solution.

The prepared solution was sprayed using nitrogen as a carrier gas onto the Mo-SLG which had a nominal temperature of 350 °C. The spraying time, the solution flow rate and the distance between the nozzle and the substrate were optimized to produce dense and crack-free Cu_2SnS_3 layers.

The Cu_2SnS_3 precursor layers were further annealed in a tube furnace in chalcogen atmosphere. More precisely, the samples were placed inside a quasi-closed graphite box filled with elemental sulfur and SnS and annealed at 550 °C for 30 min.

The surface and cross-section morphology of the Cu_2SnS_3 layers were characterized by scanning electron microscopy (FEI Helios Nanolab 600i SEM/FIB).

The structural properties of the Cu_2SnS_3 layers were analyzed by X-ray diffraction (XRD) (Panalytical X'pert Pro diffractometer with a CuKα radiation at 40 kV and 40 mA) and Raman spectroscopy (Raman, Jobin–Yvon LabRAM Aramis) by means of a green laser with an excitation wavelength of 532 nm (laser power = 3 mW) and a spot size of approximately 1 μm.

After the absorber fabrication, the solar cells were completed by a wet-chemically processed CdS buffer layer, a sputtered i-ZnO layer and a sputtered ZnO:Al front contact. An Al/Ni grid is evaporated on top of the device to improve the current collection.

Current-voltage characteristics were measured under standard test conditions using a four wire configuration. A Keithley 2400 source measuring unit under simulated AM 1.5 solar irradiation with a solar simulator (class AAA) at 100 mW/cm^2 was used. The active area of the solar cells is approximately 0.35 cm^2. Air annealing treatment of 150 s of the complete Cu_2SnS_3 device was performed at 250 °C. As a last step the cells were scribed to a reduced cell area of approximately 0.2 cm^2.

3. Results and discussion

3.1. Structural investigations

X-ray diffractograms of the as-prepared Cu_2SnS_3 before and after annealing to 550 °C are presented in Fig. 1. The as-prepared film was deposited at 350 °C. Three major peaks at 28, 47, 56° are observed consistent with all major polymorphic forms of Cu_2SnS_3. However, the absence of minor peaks means the exact polymorph cannot be determined. This is consistent with the low growth temperature which is far from the melting point (837 °C) leading to low crystalline quality. After annealing we observe a higher number of Bragg peaks than on the as-prepared films. The majority of these extra peaks appear to relate only to the monoclinic polymorph of Cu_2SnS_3. This is consistent with some of the co-authors' previous study where it was reported that the monoclinic polymorph is found above annealing temperatures of 520 °C [17]. This polymorph was shown in this study by photoluminescence measurements to be the least defective, and thus the most promising for photovoltaic applications.

Raman spectroscopy is a complementary and necessary analysis technique to XRD in the study of Cu_2SnS_3 films, enabling more insight on the crystallographic structure, as Raman shows higher sensitivity to
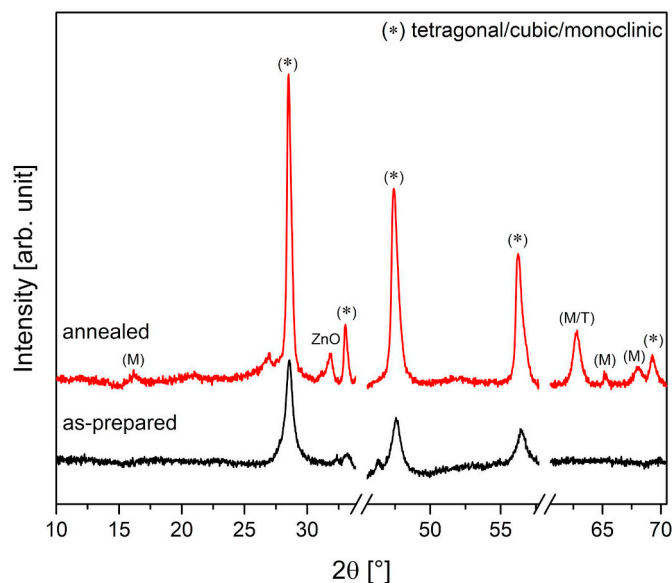

Fig. 1. XRD of the as-prepared (black) and annealed (red) Cu_2SnS_3 films. The abscissa is broken twice to focus attention onto the Cu_2SnS_3 and to remove the ZnO related peaks from the top window layers of the device. The Bragg peaks assigned with (∗) are found in all tetragonal I-43 m, cubic F-43 m and monoclinic Cc reference patterns (PDF 04–009-7947, 01–089-2877, 04–010-5719, respectively). The peak assigned to (M/T) is only found in monoclinic and tetragonal patterns while the (M) peaks are only found in the monoclinic pattern. (For interpretation of the references to colour in this figure legend, the reader is referred to the web version of this article.)
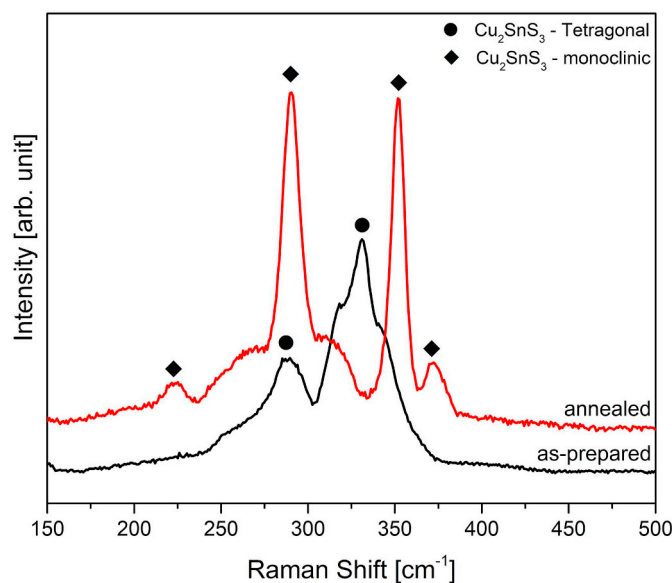

Fig. 2. Raman spectra of the as-prepared (black) and annealed (red) Cu_2SnS_3 films. Modes are assigned to the tetragonal and monoclinic polymorph of Cu_2SnS_3. (For interpretation of the references to colour in this figure legend, the reader is referred to the web version of this article.)

the different polymorphs [18–20]. Fig. 2 shows the Raman spectra measured on the Cu_2SnS_3 films as-prepared and after annealing to 550 °C. The as-prepared film shows peaks at approximately 290, 335 and 345 cm^{-1} assigned to tetragonal polymorph [21,22] with an additional peak shoulder around 318 cm^{-1} which is likely a SnS related phase [23]. The Raman spectra refine the results obtained by the XRD by confirming a single monoclinic phase of Cu_2SnS_3 after annealing showing the monoclinic Raman modes at 225, 291, 352 and 371 cm^{-1}
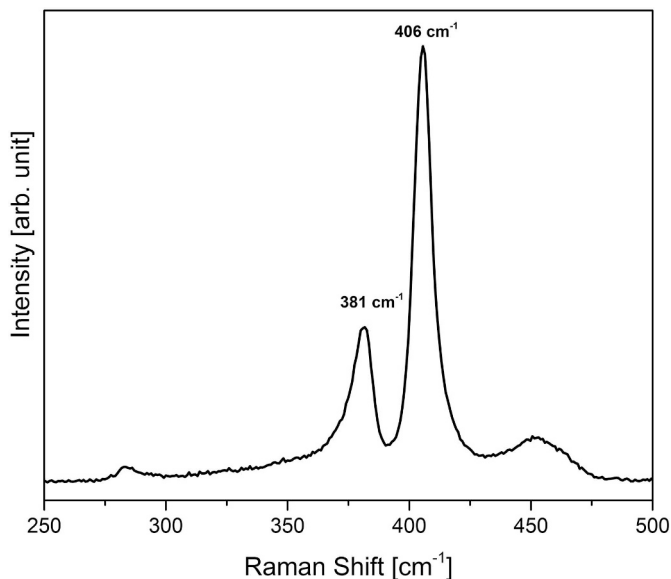
Fig. 3. Raman spectra of the annealed sample measured on the Mo back contact side after peeling off the Cu_2SnS_3 layer.

[19]. Thus, these results show the transition of a major tetragonal polymorph at 350 °C to a monoclinic polymorph, by the annealing step at 550 °C.

Raman measurement was also performed on the Mo back contact side of the annealed sample after peeling off the absorber layer and probing the remaining surface and is presented in Fig. 3. Two strong Raman modes are observed at 381 and 406 cm^{-1}, which correspond to reported Raman modes of MoS_2 [24], suggesting the Mo substrate also reacts with Sulfur during the annealing process similar to kesterite [25]. MoS_2 was previously suggested as a fair back contact to avoid decomposition of the Cu_2SnS_3 ternary into binaries [26].

3.2. Morphological investigations

Representative surface and cross section SEM images of the as-prepared and annealed Cu_2SnS_3 layers are shown in Fig. 4. The top surface (Fig. 4(a)) and cross section (Fig. 4(b)) morphology of the as-prepared Cu_2SnS_3 layers showed the films to have crack-free smooth surfaces, to consist of fine grains around 50 nm in size which make up layers of approximately 1 μm thickness, and to have small voids scattered randomly throughout the film. After annealing in sulfur and SnS,

the Cu_2SnS_3 surface consists of angular compact grains (Fig. 4(c)) ranging from approximately 200 nm to the micrometer range, whereas a larger grain structure has previously been reported to be beneficial for the absorber transport properties in annealed Cu_2SnS_3 devices [27].

3.3. Photovoltaic device

The current density-voltage (J–V) characteristics of the prepared Cu_2SnS_3 devices are shown in Fig. 5. The resulting device obtained from the as-prepared Cu_2SnS_3 showed no photovoltaic activity (not shown here), which might be attributed to the small grain structure of the as-prepared layer and the coexistence of different Cu_2SnS_3 polymorphs. The Cu_2SnS_3 device obtained from the annealed layer yielded a power conversion efficiency (PCE) of 0.65% with an open circuit voltage (V_{OC}), a short circuit current density (J_{SC}) and a fill factor (FF) of 109 mV, 17.7 mA/cm^2 and 34%, respectively as tabulated in the inset in Fig. 5. All current voltage (J-V) parameters are rather low here. The morphological inhomogeneity, defects and the presence of MoS_2 may account for the low device performance. Also, the much reduced JV values here could be partly due to the absorber layer only being 1 μm thick. A short annealing at 250 °C carried out in air for 150 s of the aforementioned device led to an overall improvement in current voltage parameters of the Cu_2SnS_3 device. The air annealed device showed an efficiency of 1.94%. Previously air annealing on completed Cu_2SnS_3 devices in air has been shown to improve both the diffusion length and depletion width inside of the absorber layer. Here air annealing showed significant improvement in J_{SC}, V_{OC} and FF as given in Fig. 5 inset table, which is consistent with better collection lengths and less recombination [28]. Possible shunt paths were mechanically removed leading to a significant increase in FF to 53% yielding a Cu_2SnS_3 device with 2.28% efficiency, which is the highest achieved device efficiency for a Cu_2SnS_3 absorber obtained from chemical spray pyrolysis.

4. Conclusion

A water-based chemical spray pyrolysis process was employed to prepare Cu_2SnS_3 layers followed by an annealing step in chalcogen atmosphere at high temperature. The influence of the annealing step on the structural, morphological and photovoltaic properties of the Cu_2SnS_3 layers was studied. The as-prepared Cu_2SnS_3 layers exhibited a tetragonal structure of crack-free and fine grain structure. *Re*-crystallization and structural phase transition into monoclinic Cu_2SnS_3 structure was observed due to the annealing process.

The overall device performance was found to be improved upon air annealing where the device efficiency increased from 0.65% to 1.94%. The best achieved efficiency by this process reached 2.28% on an area of 0.2 cm^2.
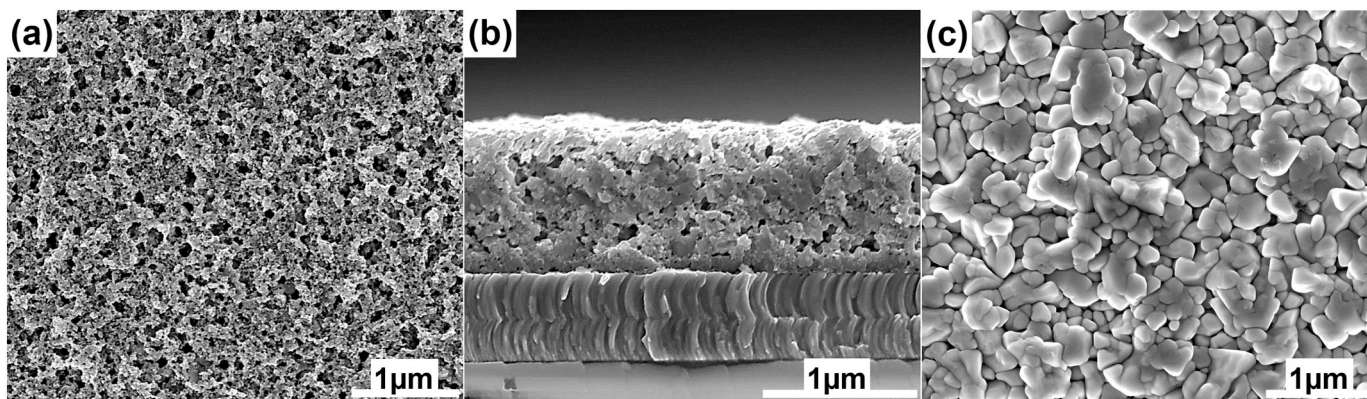

Fig. 4. SEM images of Cu_2SnS_3 layers: (a and b) top view and cross section of as-prepared layer respectively, (c) top view of the annealed layer.

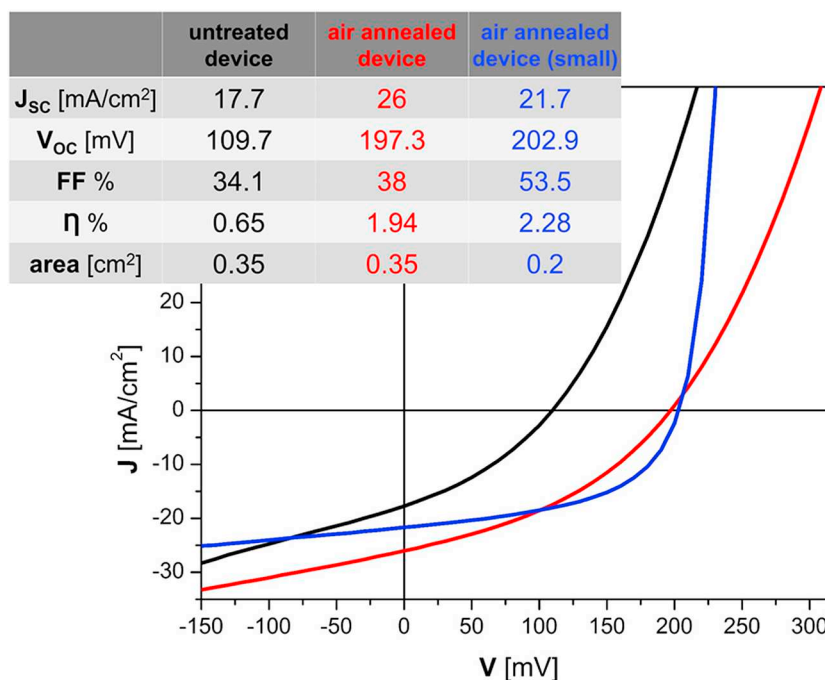|	untreated device	air annealed device	air annealed device (small)
J_{SC} [mA/cm^2]	17.7	26	21.7
V_{OC} [mV]	109.7	197.3	202.9
FF %	34.1	38	53.5
η %	0.65	1.94	2.28
area [cm^2]	0.35	0.35	0.2

Fig. 5. J–V characteristics of the prepared Cu_2SnS_3 devices: as-prepared (black), air annealed (red) and air annealed after removing shunt paths (blue). (For interpretation of the references to colour in this figure legend, the reader is referred to the web version of this article.)

Acknowledgement

References

[1] ZSW Sets New World Record for Thin-film Solar Cells - CIGS PV's efficiency ratings rising fast, https://www.zsw-bw.de/fileadmin/user_upload/PDFs/Pressemitteilungen/2016/pr09-2016-ZSW-WorldRecordCIGS.pdf, (2016) (accessed 03 July 2018).
[2] Solar Frontier Achieves World Record Thin-Film Solar Cell Efficiency of 22.9%, http://www.solar-frontier.com/eng/news/2017/1220_press.html, (2017) (accessed 03 July 2018).
[3] W. Wang, M.T. Winkler, O. Gunawan, T. Gokmen, T.K. Todorov, Y. Zhu, D.B. Mitzi, Device Characteristics of CZTSSe Thin-Film Solar Cells with 12.6% Efficiency, Adv. Energy Mater. 4 (2014) 1301465.
[4] S. Siebentritt, S. Schorr, Kesterites-a challenging material for solar cells, Prog. Photovolt. Res. Appl. 20 (2012) 512–519.
[5] S. Bourdais, C. Choné, B. Delatouche, A. Jacob, G. Larramona, C. Moisan, A. Lafond, F. Donatini, G. Rey, S. Siebentritt, A. Walsh, G. Dennler, Is the Cu/Zn Disorder the Main Culprit for the Voltage Deficit in Kesterite Solar Cells? Adv. Energy Mater. 6 (2016) 1502276.
[6] D.M. Berg, R. Djemour, L. Guetay, G. Zoppi, S. Siebentritt, P.J. Dale, Thin film solar cells based on the ternary compound Cu_2SnS_3, Thin Solid Films 520 (2012) 6291–6294.
[7] P.A. Fernandes, P.M.P. Salome, A.F. da Cunha, A study of ternary Cu_2SnS_3 and Cu_3SnS_4 thin films prepared by sulfurizing stacked metal precursors, J. Phys. D. Appl. Phys. 43 (2010) 215403.
[8] N. Aihara, H. Araki, A. Takeuchi, K. Jimbo, H. Katagiri, Fabrication of Cu_2SnS_3 thin films by sulfurization of evaporated Cu-Sn precursors for solar cells, Phys. Status Solidi C 10 (2013) 1086–1092.
[9] M. Bouaziz, M. Amlouk, S. Belgacem, Structural and optical properties of Cu_2SnS_3 sprayed thin films, Thin Solid Films 517 (2009) 2527–2530.
[10] A. Kanai, K. Toyonaga, K. Chino, H. Katagiri, H. Araki, Fabrication of Cu_2SnS_3 thin film solar cells with power conversion efficiency over 4%, Jpn. J. Appl. Phys. 54 (2015) 08KC06.
[11] M. Nakashima, J. Fujimoto, T. Yamaguchi, M. Izaki, Cu_2SnS_3 thin-film solar cells fabricated by sulfurization from NaF/Cu/Sn stacked precursor, Appl. Phys. Express 8 (2015) 042303.
[12] J. Koike, K. Chino, N. Aihara, H. Araki, R. Nakamura, K. Jimbo, H. Katagiri, Cu_2SnS_3 thin-film solar cells from electroplated precursors, Jpn. J. Appl. Phys. 51 (2012) 10NC34.
[13] G. Sunny, T. Thomas, D.R. Deepu, C.S. Kartha, K.P. Vijayakumar, Thin film solar cell using earth abundant Cu_2SnS_3 (CTS) fabricated through spray pyrolysis:

Influence of precursors, Optik - International Journal for Light and Electron Optics 144 (2017) 263–270.
[14] Y.-X. Guo, W.-J. Cheng, J.-C. Jiang, J.-H. Chu, The effect of substrate temperature, Cu/Sn ratio and post-annealing on the phase-change and properties of Cu_2SnS_3 film deposited by ultrasonic spray pyrolysis, J. Mater. Sci. Mater. Electron. 27 (2016) 4636–4646.
[15] B. Patel, M. Waldiya, A. Ray, Highly phase-pure spray-pyrolysed Cu_2SnS_3 thin films prepared by hybrid thermal treatment for photovoltaic applications, J. Alloys Compd. 745 (2018) 347–354.
[16] E.V.C. Robert, J. De Wild, P.J. Dale, Reaction chemistry of group IV copper chalcogenide semiconductors Cu_2MX_3 (M = Sn, Ge and X = S, Se), J. Alloys Compd. 695 (2017) 1307–1316.
[17] J. de Wild, E.V.C. Robert, B.E. Adib, D. Abou-Ras, P.J. Dale, Secondary phase formation during monoclinic Cu_2SnS_3 growth for solar cell application, Sol. Energy Mater. Sol. Cells 157 (2016) 259–265.
[18] D.M. Berg, R. Djemour, L. Guetay, S. Siebentritt, P.J. Dale, X. Fontane, V. Izquierdo-Roca, A. Perez-Rodriguez, Raman analysis of monoclinic Cu_2SnS_3 thin films, Appl. Phys. Lett. 100 (2012) 192103.
[19] E.V.C. Robert, R. Gunder, J. de Wild, C. Spindler, F. Babbe, H. Elanzeery, B. El Adib, R. Treharne, H.P.C. Miranda, L. Wirtz, S. Schorr, P.J. Dale, Synthesis, theoretical and experimental characterisation of thin film $Cu_2Sn_{1-x}Ge_xS_3$ ternary alloys (x = 0 to 1): homogeneous intermixing of Sn and Ge, Acta Mater. 151 (2018) 125–136.
[20] J. de Wild, E.V.C. Robert, B.E. Adib, D. Abou-Ras, P.J. Dale, Secondary phase formation during monoclinic Cu_2SnS_3 growth for solar cell application, Sol. Energy Mater. Sol. Cells 157 (2016) 259–265.
[21] D. Tiwari, T.K. Chaudhuri, T. Shripathi, U. Deshpande, V.G. Sathe, Microwave-assisted rapid synthesis of tetragonal Cu_2SnS_3 nanoparticles for solar photovoltaics, Applied Physics A 117 (2014) 1139–1146.
[22] H. Guan, H. Shen, C. Gao, X. He, Structural and optical properties of Cu_2SnS_3 and Cu_3SnS_4 thin films by successive ionic layer adsorption and reaction, J. Mater. Sci. Mater. Electron. 24 (2013) 1490–1494.
[23] P.A. Fernandes, P.M.P. Salome, A.F. da Cunha, Study of polycrystalline Cu_2ZnSnS_4 films by Raman scattering, J. Alloys Compd. 509 (2011) 7600–7606.
[24] G.L. Frey, R. Tenne, M.J. Matthews, M.S. Dresselhaus, G. Dresselhaus, Raman and resonance Raman investigation of MoS_2 nanoparticles, Phys. Rev. B 60 (1999) 2883–2892.
[25] S. Byungha, G. Oki, Z. Yu, G. Supratik Jay, Thin film solar cell with 8.4% power conversion efficiency using an earth-abundant Cu_2ZnSnS_4 absorber, Prog. Photovolt. Res. Appl. 21 (2013) 72–76.
[26] J. de Wild, E.V.C. Robert, P.J. Dale, Chemical stability of the Cu_2SnS_3/Mo interface, 2016 IEEE 43rd Photovoltaic Specialists Conference (PVSC), 2016, pp. 0428–0430.
[27] A.C. Lokhande, R.B.V. Chalapathy, M. He, E. Jo, M. Gang, S.A. Pawar, C.D. Lokhande, J.H. Kim, Development of Cu_2SnS_3 (CTS) thin film solar cells by physical techniques: a status review, Sol. Energy Mater. Sol. Cells 153 (2016) 84–107.
[28] J. de Wild, E. Kalesaki, E.V.C. Robert, P.J. Dale, Quantum efficiency measurements and modeling as tools to monitor air annealing of Cu_2SnS_3 solar cells, IEEE Journal of Photovoltaics 7 (2017) 268–272.